Phototrophic pigment diversity and picophytoplankton in permafrost thaw lakes

A. Przytulska[1,2], J. Comte[1,2,3], S. Crevecoeur[1,2,3], C. Lovejoy[1,2,3], I. Laurion[4] and W. F. Vincent[1,2]

[1]Centre d'études nordiques (CEN) and Département de biologie, Université Laval, Québec City, QC G1V 0A6, CANADA

[2]Takuvik Joint International Laboratory, Centre National de la Recherche Scientifique (France, CNRS UMI 3376) and Département de Biologie, Université Laval, Québec City, QC G1V 0A6, CANADA.

[3]Institut de Biologie Intégrative et des Systèmes (IBIS), Université Laval, Québec City, QC G1V 0A6, CANADA.

[4]Centre d'études nordiques (CEN) and Centre Eau Terre Environnement, Institut national de la recherche scientifique (INRS-ETE), Québec City, QC G1K 9A9, CANADA

Running title: Phototrophs in subarctic thaw lakes

Keywords: lakes; permafrost; phytoplankton; picocyanobacteria; picoeukaryotes; autotrophic picoplankton; pigments; protists; thermokarst

Biogeosciences special issue: 'Freshwater ecosystems in changing permafrost landscapes'.

Abstract

Permafrost thaw lakes (thermokarst lakes) are widely distributed across the northern landscape, and are known to be biogeochemically active sites that emit large amounts of carbon to the atmosphere as CH_4 and CO_2. However, the abundance and composition of the photosynthetic communities that consume CO_2 have been little explored in this ecosystem type. In order to identify the major groups of phototrophic organisms and their controlling variables, we sampled 12 permafrost thaw lakes along a permafrost degradation gradient in northern Québec, Canada. Additional samples were taken from 5 rock-basin reference lakes in the region to determine if the thaw lakes differed in limnological properties and phototrophs. Phytoplankton community structure was determined by high performance liquid chromatography analysis of their photoprotective and photosynthetic pigments, and autotrophic picoplankton concentrations were assessed by flow cytometry. One of the black colored lakes located in a landscape of rapidly degrading palsas (permafrost mounds) was selected for high-throughput 18S rRNA sequencing to complement conclusions based on the pigment and cytometry analyses. The results showed that the limnological properties of the thaw lakes differed significantly from the reference lakes, and were more highly stratified. However, both waterbody types contained similarly diverse phytoplankton groups, with dominance of the pigment assemblages by fucoxanthin-containing taxa, as well as chlorophytes, cryptophytes and cyanobacteria. Chlorophyll *a* concentrations (Chl *a*) were correlated with total phosphorus (TP), and both were significantly higher in the thaw lakes (overall means of 3.3 µg Chl *a* L^{-1} and 34 µg TP L^{-1}) relative to the reference lakes (2.0 µg Chl *a* L^{-1} and 8.2 µg TP L^{-1}). Stepwise multiple regression of Chl *a* against the other algal pigments showed that it was largely a function of alloxanthin, fucoxanthin and Chl *b* ($R^2 = 0.85$). The bottom waters of two of the thaw lakes also contained high concentrations of bacteriochlorophyll *d*, showing the presence of green photosynthetic sulphur bacteria. The

molecular analyses indicated a relatively minor contribution of diatoms, while chrysophytes, dinoflagellates and chlorophytes were well represented; the heterotrophic eukaryote fraction was dominated by numerous ciliate taxa, and also included Heliozoa, Rhizaria, chytrids and flagellates. Autotrophic picoplankton occurred in biovolume concentrations up to 3.1×10^5 μm^3 mL^{-1} (picocyanobacteria) and 1.9×10^6 μm^3 mL^{-1} (picoeukaryotes), and varied greatly among lakes. Both groups of picophytoplankton were positively correlated with total phytoplankton abundance, as measured by Chl *a*; picocyanobacteria were inversely correlated with dissolved organic carbon, while picoeukaryotes were inversely correlated with conductivity. Despite their net heterotrophic character, subarctic thaw lakes are rich habitats for diverse phototrophic communities.

1 Introduction

Degradation of ice-rich permafrost leads to the formation of thaw lakes, which are among the most abundant aquatic habitats in high latitude regions (Pienitz et al., 2008; Jones et al., 2012). These environments have attracted increasing scientific interest because of their biogeochemical reactivity. However, although there is rapidly increasing knowledge about their role in greenhouse gas (GHG) emissions (Laurion et al., 2010; Walter et al., 2006), little is known about their photosynthetic communities. Phototrophic organisms consume CO_2 and thereby reduce the net emission to the atmosphere; however, few studies have examined phytoplankton or other phototrophs in these abundant waters. Early studies in the U.S. Tundra Biome Program at Barrow, Alaska, recorded 105 species of algae in tundra lakes and ponds, with dominance of cryptophytes and chrysophytes (Alexander et al., 1980). More recent studies have focused on thaw lake diatoms as paleolimnological indicators, but the dominants in these records are often benthic taxa such as *Pinnularia* and *Fragilaria* (Bouchard et al., 2013). A lake survey in the western Hudson Bay lowlands, including in permafrost catchments, showed that the phytoplankton had diverse communities, primarily composed of cyanobacteria, chrysophytes, chlorophytes, cryptophytes, dinoflagellates and diatoms (Paterson et al., 2014).

Picophytoplankton (PP), consisting of picocyanobacteria and picoeukaryotes (nominally defined as cells 1 to 3 μm in diameter), contribute a major fraction of the total phototrophic biomass across a wide range of aquatic ecosystems (Richardson and Jackson, 2007), including northern lakes and rivers (Waleron et al., 2007; Vallières et al., 2008). In subarctic (Bergeron and Vincent, 1997) and high arctic (van Hove et al., 2008) lakes, picocyanobacteria may dominate the phytoplankton community in terms of biomass as well as cell abundance. For example, in

77 large oligotrophic Clear Water Lake (Lac à l'eau claire, Nunavik, Canada), small cell
78 phytoplankton (cell fraction that passed through a 2 μm filter) accounted for 75% of the total
79 phytoplankton Chl *a* (Bergeron and Vincent, 1997). However, the suitability of permafrost thaw
80 lakes as a habitat for picophytoplankton has not been explored.
81
82 Our overall aim in the present study was to evaluate the major groups of phytoplankton in
83 subarctic thaw lakes, and to relate this abundance and community structure to environmental
84 variables. For this we employed phototrophic pigment analysis by high performance liquid
85 chromatography (HPLC), an approach that has been applied with success to describe
86 phytoplankton community structure at the phylum level in a wide range of freshwater (e.g., Fietz
87 and Nicklisch, 2004) and marine (e.g., Ansotegui et al., 2001) studies.
88
89 A secondary objective was to determine the abundance and distribution of picocyanobacteria and
90 picoeukaryotes. As a further guide to the composition of the eukaryotic plankton, and in support
91 of the pigment and picoeukaryote observations, we also applied high throughput 18S rRNA
92 sequencing to surface and bottom waters from one selected lake that was strongly influenced by
93 permafrost degradation. Our study included a wide range of small lakes across the gradient of
94 permafrost degradation in Subarctic Quebec, Canada, from sporadic permafrost landscapes in the
95 south (less than 10% of the area containing permafrost) to discontinuous permafrost in the north
96 (10-90% permafrost). We also took comparative samples from a set of shallow rock-basin lakes
97 that are unaffected by thermokarst processes. Given their limnological variability, as indicated by
98 the variety of water colors among thaw lakes, we hypothesized that there would be large
99 variations in total phytoplankton pigment concentration, pigment diversity and

100 picophytoplankton biovolume. Degrading permafrost soils release dissolved organic carbon
101 (DOC) and fine inorganic particles into the thaw lakes, and these constituents determine the
102 attenuation of light down the water column and the variability in color (Watanabe et al., 2011).
103 DOC also influences the near surface thermal and stratification regime (Caplanne and Laurion,
104 2008), and temperature is known to exert a direct effect on phytoplankton community structure,
105 particularly favouring cyanobacterial dominance (Paerl and Huisman, 2008). We therefore
106 hypothesised that DOC and temperature would be the primary drivers of variations in
107 phytoplankton pigmentation and picophytoplankton biovolume.
108

109 **2 Materials and Methods**

110 **2.1 Study Sites**

111 Twelve thaw lakes (small perennial waterbodies created by thermokarst erosion of the
112 permafrost) were sampled in subarctic Québec during the period of warm open-water conditions,
113 in August 2011 and 2012 (Table S1). The lakes were distributed along a north-south permafrost
114 degradation gradient and across four geographically distinct locations: the Sasapimakwananisikw
115 River valley (SAS) and the Kwakwatanikapistikw River valley (KWK) near Whapmagoostui-
116 Kuujjuarapik; and the Sheldrake River valley (BGR) and the Nastapoka River valley (NAS) near
117 Umiujaq. The KWK and SAS valleys occur within the sporadic permafrost landscape, while the
118 BGR and NAS valleys are located in the discontinuous permafrost landscape (Fig. 1). Each
119 valley is characterised by distinct vegetation cover and soil structure. Lakes located within the
120 KWK valley are situated on impermeable clay-silt beds where the drainage basin is covered with
121 dense shrub vegetation (Breton et al., 2009), whereas lakes in the SAS valley are located in
122 peatlands in which permafrost mounds (palsas) are thawing and degrading rapidly (Bhiry et al.,

123 2011). The lakes located in the northern valleys (BGR, NAS) are situated on marine clay-silt
124 beds and are surrounded by forest and shrub tundra. In addition to twelve permafrost thaw lakes,
125 a set of five shallow rock-basin lakes (SRB) located on basalt bedrock was sampled in the
126 vicinity of Whapmagoostui-Kuujjuarapik. These provided a set of reference lakes that are
127 located at the same latitude and climatic setting, but without the direct influence of degrading
128 permafrost that is experienced by the thaw lakes. The dates of sampling are given in Table S1.
129

130 **2.2 Physicochemical analyses**

131 Profiles of temperature, dissolved oxygen, conductivity, and pH of the 17 lakes were recorded
132 with a 600R multiparametric probe (Yellow Springs Instrument Co.). Additionally temperature
133 and conductivity were recorded with RBR XR620 conductivity-temperature-depth profiler
134 (Richard Brancker Research Ltd). Near surface water samples (0.2 m depth) were collected into
135 dark polyethylene bottles, previously washed with 10% hydrochloric acid and rinsed in MQ
136 water. The samples were stored in coolers and transported to laboratory within 4 h of collection.
137 The total nitrogen (TN) and total phosphorus (TP) measurements were performed on unfiltered
138 water samples collected in 125ml bottles, acidified with sulfuric acid (0.2% final concentration),
139 and stored at 4°C until persulfate digestion. TN concentrations were then measured with a Lachat
140 flow injection analyzer and TP concentrations were measured using a Genesys 10UV
141 spectrophotometer (Thermo Spectronic) and standard techniques (Stainton et al., 1977). Total
142 suspended solids (TSS) were collected onto pre-combusted and pre-weighed glass fiber filters
143 (Advantec MFS) that were dried for 2 h at 60°C and weighed on a Sartorius high precision
144 balance. Dissolved organic carbon (DOC), colored dissolved organic matter (CDOM), soluble
145 reactive phosphorus (SRP) and nitrate (NO_3^-) measurements were performed on water filtered

through 0.2 μm cellulose acetate filters (Advantec MFS). Samples for DOC analyses were stored in 45 mL dark glass bottles that had been previously burned at 450°C for 4 h and rinsed with MQ water to remove any traces of organic substances. The DOC analysis was with a Shimadzu TOC-5000A carbon analyzer calibrated with potassium biphthalate. CDOM was determined by spectrophotometric absorbance of the filtrates at 320 nm, blanked against filtered MQ water and converted to absorption values. SRP and NO_3^- were measured in the filtrates using standard colorimetric methods (Stainton et al., 1977), and major ions were measured using Dionex ICS 2000 ion chromatograph.

2.3 Pigment analysis

Near surface (0.2 m depth) and near-bottom water samples (0.2 m above sediments; 50-500 mL) from each lake were filtered onto 25-mm diameter GF/F glass-fibre filters, and immediately frozen and stored at -80°C until pigment extraction in methanol. Pigments were analyzed by high performance liquid chromatography (HPLC) following the protocols and standards described in Bonilla et al. (2005). For some of the statistical analyses, two groups of algal accessory pigments were separated as in Bonilla et al. (2005): photoprotective pigments (canthaxanthin, diadinoxanthin, echinenone, lutein, violaxanthin and zeaxanthin) and light harvesting, photosynthetic pigments (alloxanthin, Chl *b*, fucoxanthin and peridinin). Standards for identification and quantification of pigments (Chl *a*, Chl *b*, Chl *c2*, alloxanthin, β,β-carotene, canthaxanthin, crocoxanthin, diadinoxanthin, echinenone, fucoxanthin, lutein, peridinin, violaxanthin, and zeaxanthin) were obtained from Sigma Inc. (St. Louis, MO, USA) and DHI Water & Environment (Hørsholm, Denmark) to calibrate the HPLC. The photodiode array spectrum of each peak was checked against the reference spectra in Roy et al. (2011). No

169 standards were available for bacteriochlorophyll *d* and the main chromatogram peaks for this
170 pigment at 430 nm were expressed as Chl *a* equivalent concentrations.
171
172 **2.4 Picophytoplankton enumeration**
173 Near surface (0.2 m depth), unfiltered water samples from each lake were transferred to 5mL
174 Cryovials, fixed with glutaraldehyde (10% final concentration) and stored at -80°C until analysis
175 for picophytoplankton abundance. The cells were enumerated using a Becton Dickinson flow
176 cytometer (BD FacsCalibur), equipped with an argon laser. Analyses were done at the lowest
177 flow rate (12 μL min^{-1}), using a solution of 1-μm diameter, yellow-green microspheres
178 (Polysciences, Inc.) as an internal standard. Bead concentrations in the calibration solution were
179 controlled using TrueCountAbsolute counting tubes (BD Biosciences). Picocyanobacteria and
180 picoeukaryotes were distinguished based on their chlorophyll and phycoerythrin fluorescence.
181 Detection of the two groups was performed by the comparison of flow cytograms where cells
182 were discriminated based on their side scatter signals (SSC) and both red (FL3) and orange
183 fluorescence (FL2) as well as FL3 versus FL2. The cytograms were analyzed using the Cell
184 Quest Pro software, with manual gating to discriminate the different populations. For the
185 picophytoplankton biovolume estimates, the diameters of 20 cells of each group in a sample
186 from thaw lake KWK12 were measured under epifluorescence microscopy at 1000x
187 magnification, and were then converted to spherical biovolumes. The measured cell diameters
188 (±SD) were 1.0 ± 0.2 μm for picocyanobacteria and 2.0 ± 0.5 μm for picoeukaryotes, giving
189 biovolumes per cell of 0.52 and 4.19 μm^3, respectively.
190
191

192 **2.5 RNA sampling and analysis**

193 Water samples from the near surface (0.2 m depth) and near-bottom (0.2 m above sediments) of
194 the black palsa lake SAS2A were first prefiltered through a 20 µm mesh to remove larger
195 organisms and then filtered sequentially through a 3 µm pore size, 47 mm diameter
196 polycarbonate filter (DHI) and a 0.2 µm Sterivex unit (Millipore) with a peristaltic pump. From
197 100 to 300 mL of water were filtered and the filtration was stopped after 2 hours to minimize
198 RNA degradation. The 3 µm filter for larger cells (L fraction) and the 0.2 µm filter for the
199 smaller fraction (S fraction) were both preserved in RNAlater (Life Technologies) and then
200 stored at -80°C until extraction.
201
202 Samples were extracted with the AllPrep DNA/RNA Mini Kit (Qiagen). This protocol was
203 modified by the addition of cross-linked polyvinylpyrrolidone (PVP, Alfa Aesar) (UV light
204 sterilized) to a final concentration of 10% before loading the samples onto the lysate
205 homogenization column. For all samples, the extracted RNA was converted to cDNA
206 immediately with a High Capacity cDNA Reverse Transcription Kit (Applied Biosystems-
207 Ambion) and stored at -80°C until analysis. The V4 region of the eukaryotic 18S rRNA that had
208 been converted to cDNA was amplified using the 454 primers as described in Comeau et al.
209 (2011). PCR was carried out in a total volume of 50 µL, the mixture contained HF buffer 1X
210 (NEB), 0.25 µM of each primer, 200 µM of each dNTPs (Life Technology), 0.4 mg mL^{-1} BSA
211 (NEB), 1 U of Phusion High-Fidelity DNA polymerase (NEB) and 1 µL of template cDNA. Two
212 more reactions with 5X and 10X diluted template were also carried out for each sample, to
213 minimize potential primer bias. Thermal cycling began with an initial denaturation at 98°C for
214 30 s, followed by 30 cycles of denaturation at 98°C for 10 s, annealing at 55°C for 30 s,

extension at 72°C for 30 s and a final extension at 72°C for 270 s. The three dilution reactions were pooled and purified with a magnetic bead kit Agencourt AMPure XP (Beckman Coulter) and then quantified spectrophotometerically with the Nanodrop 1000 (Thermo Fisher Scientific). The amplicons were sequenced on 1/8 plates of the Roche 454 GS-FLX using the "PLUS" chemistry at the IBIS/Laval University, Plate-forme d'analyses génomiques (Québec City, QC). The reads have been deposited in the NCBI short read archive as SRP060634.

Sequences were analysed using the UPARSE pipeline (Edgar, 2013). For quality filtering, the sequences were truncated at 245 bp to keep 50% of the reads at the 0.5 expected error rate. Singletons as well as chimeras were then removed and operational taxonomic units (OTUs) were determined at the ≥ 98% similarity level. These OTUs were classified using the mothur classifier (Schloss et al., 2009) with a 0.8 confidence threshold based on the SILVA reference database (Pruesse et al., 2007) modified to include sequences from our in-house, curated northern 18S rRNA gene sequence database (Lovejoy et al., 2015). In order to compare samples, the OTU tables were each subsampled 100 times at 2200 reads, which corresponded to the lowest number of reads per sample minus 10%; this subsampling used the command multiple_rarefaction_even_depth.py in QIIME (Caporaso et al., 2010). The most abundant and unclassified OTUs were subsequently submitted to a BLASTn search to the nr database in NCBI GenBank (http://blast.ncbi.nlm.nih.gov/Blast.cgi) to identify the nearest match.

2.6 Statistical analysis

The normal distribution of environmental variables was tested using the Kolmogorov-Smirnov test, and right-skewed variables were normalized by natural logarithm transformation. Given the

238 order of magnitude differences in picophytoplankton abundances and pigment concentrations
239 among samples, the HPLC and flow cytometry data were also normalized by logarithmic
240 transformation. Correlations within and among the phytoplankton, pigment and environmental
241 variables were tested by Pearson correlation analysis, with correction for multi-testing using the
242 false discovery rate procedure as in Benjamini and Hochberg (1995). To investigate the extent to
243 which environmental variables drove the distribution of pigment diversity among the different
244 water bodies, a redundancy analysis (RDA, Legendre and Legendre, 2012) was run. This was
245 based on Bray-Curtis distances for the pigment matrix (db-RDA) and the data were log-
246 transformed prior to analysis. The significance of the model was assessed via 1000 permutations,
247 and the analysis was performed in RStudio (version 0.98.501) using the Vegan package
248 (Oksanen et al., 2015). Stepwise multiple linear regression models were performed using Past
249 3.04, with secondary cross-correlated variables removed prior to analysis.
250
251 **3 Results**
252 **3.1 Environmental heterogeneity**
253 The thaw lakes spanned a wide range of environmental conditions, including water color and
254 CDOM, with the latter strongly correlated with DOC ($R = 0.67$, $p < 0.0001$). The highest DOC
255 concentrations (up to 17 mg L^{-1}) and CDOM (up to 117 m^{-1}) were recorded in the SAS lakes
256 (Table 1). These waters were black in color and also had the lowest pH values (6.0 – 6.6). The
257 highest total nutrient concentrations (up to 125 µg TP L^{-1} and 4 mg TN L^{-1}) were recorded in
258 lakes located within the KWK and NAS valleys, and the values were lowest in the shallow rock-
259 basin waters (minima of 1.6 µg TP L^{-1} and 0.1 mg TN L^{-1}). Nitrogen to phosphorus ratios varied
260 greatly among the 17 lakes, from 4 to 131 (g g^{-1}), and total suspended solids were similarly

261 variable, from 1 to 320 mg L^{-1} (Table 1). The NAS valley waters contained especially high
262 concentrations of suspended clay particles, producing an opaque milky appearance. Despite their
263 shallowness and small size, the thaw lakes were highly stratified in terms of temperature and
264 oxygen (Fig. 2), with anoxic bottom waters in the SAS and KWK lakes. Some had pronounced
265 thermal gradients, with temperature differences up to 10°C between the surface and bottom
266 waters. In contrast, the reference lakes showed more homogenous conditions, indicative of
267 mixing (Fig. 2).
268
269 **3.2 Planktonic pigments**
270 Phytoplankton abundance, as measured by Chl *a* concentrations, varied greatly among the
271 waterbodies (Table 1), from 0.4 (SRB1) to 6.8 (KWK6) µg L^{-1} in 2011 and from 0.2 (SRB1) to
272 9.1 (KWK1) µg L^{-1} in 2012. There was also a small but significant difference in Chl *a*
273 concentrations between years, with means of 3.7 and 2.6 µg L^{-1}, respectively (paired t-test,
274 $t = 2.5$, $p = 0.02$). On average, Chl *a* was significantly higher in the thaw lakes than the reference
275 rock-basin waters: the overall means were 3.3 and 2.0 µg Chl *a* L^{-1}, respectively.
276
277 The pigment analyses of the phytoplankton (Table 2) showed that there were diverse
278 communities including fucoxanthin-containing groups (potentially diatoms, chrysophytes and
279 certain dinoflagellates), chlorophytes (Chl *b*, lutein and violaxanthin), cryptophytes
280 (alloxanthin), dinoflagellates (peridinin) and cyanobacteria (zeaxanthin, canthaxanthin,
281 echinenone). The pigments Chl c_1, c_2, c_3 and crocoxanthin were also present, but generally at
282 trace concentrations, and only in certain lakes. The abundance of cyanobacterial populations in
283 KWK, BGR and NAS lakes was indicated by high concentrations of zeaxanthin (e.g., NASH)

284 and echinenone (SRB3). The KWK lakes had high concentrations of zeaxanthin (up to 0.7 nmol
285 L^{-1} in KWK23), accompanied by high concentrations of fucoxanthin and green algal pigments
286 (lutein and violaxanthin), as well as high concentrations of diadinoxanthin (e.g., KWK1). In the
287 SAS lakes, a dominance of dinoflagellates was indicated by high concentrations of peridinin.
288 Echinenone was present in KWK and SRB lakes and high concentrations of violaxanthin were
289 also recorded in BGR lakes. Fucoxanthin-groups were abundant in SRB and SAS as well as in
290 NASH and BGR2. The turbid thaw lakes within the NAS valley had high concentrations of β,β-
291 carotene. Relatively high levels of ancillary photosynthetic pigments were present in NASA and
292 SAS lakes as well as in some waters of shallow rock-basin lakes (Table 2). Photoprotective
293 pigments were relatively more abundant in KWK lakes (notably KWK1 and KWK6) as well as
294 in the SRB waters (violaxanthin), and less abundant in the DOC-rich SAS lakes (Table 2). The
295 bottom waters of the thaw lakes also contained diverse planktonic pigments, including high
296 levels of diadinoxanthin and alloxanthin in KWK lakes, fucoxanthin in BGR2 and Chl *b* in SRB
297 lakes. High levels of bacteriochlorophyll *d* indicating abundant populations of green
298 photosynthetic sulfur bacteria were recorded in the deeper, anoxic waters of KWK lakes (Table
299 3, Fig. 3).
300
301 For the overall data set, Chl *a* concentrations were significantly correlated with TP ($R = 0.47$;
302 $p = 0.05$), and with TSS ($R = 0.55$; $p = 0.03$), which were themselves strongly correlated
303 ($R = 0.87$; $p < 0.0001$). A forward stepwise linear regression showed that Chl *a* was best
304 described by a combination of the accessory pigments alloxanthin ($p < 0.014$), fucoxanthin
305 ($p < 0.001$) and Chl *b* ($p < 0.001$): ln Chl *a* = 1.774 + 0.161 ln Allo + 0.380 ln Chl *b* + 0.341 ln
306 Fuco ($R^2 = 0.85$; $p < 0.001$).

307

308 Several pigments were highly cross-correlated. These included alloxanthin and lutein ($R = 0.81$,
309 $p < 0.001$) and both pigments with Chl *b* ($R = 0.71$; 0.92, $p < 0.001$). The chlorophyte pigment
310 violoxanthin was also correlated with Chl *b* ($R = 0.60$, $p < 0.001$) and fucoxanthin ($R = 0.58$,
311 $p < 0.001$). Fucoxanthin itself was most strongly correlated with diadinoxanthin ($R = 0.77$,
312 $p < 0.001$). The cyanobacterial pigments echinenone and canthaxanthin were significantly
313 correlated ($R = 0.57$, $p < 0.001$), but not with zeaxanthin ($p > 0.05$). The summations within the
314 two categories of pigments, photoprotective and photosynthetic, were also positively correlated
315 ($R = 0.63$; $p < 0.001$*).* Consistent with the multivariate analyses, the accessory pigments were
316 uncorrelated with individual environmental variables (all corrected p values were > 0.05), with
317 the exception of lutein. This chlorophyte pigment was significantly correlated with TP ($R = 0.53$;
318 $p = 0.01$), but this may simply reflect the strong correlation between lutein and Chl *a* ($R = 0.79$;
319 $p < 0.0001$), which itself correlated with TP.
320

321 The db-RDA model showed a clear separation of the different valleys in terms of phytoplankton
322 pigment composition. These distinct patterns in pigment composition was partially explained by
323 the influence of valley specific environmental variables. In addition, the results from db-RDA
324 reaffirmed the large lake-to-lake heterogeneity in each of the valleys, even among nearby lakes.
325 The first two canonical components were related to TP, DOC and pH and explained 11% of the
326 total variance in pigment composition (Fig. 4). The db-RDA model as a whole explained 16.4%
327 of the variance ($R^2 = 0.164$, $F = 1.71$, $df = 8$, $p = 0.012$).
328
329

330 **3.3 Picophytoplankton abundance and biovolume**

331 Picophytoplankton concentrations varied greatly among the lakes (Fig. 5). The
332 picocyanobacterial abundances ranged from 1.8 x 10^3 cells mL^{-1} (SAS1B) to 5.9 x 10^5 cells mL^{-1}
333 (KWK23), equivalent to biovolume concentrations of 9.5 × 10^2 (SAS1B) to 3.1 × 10^5 μm^3 mL^{-1}
334 (KWK23), while the picoeukaryote abundances ranged from 1.35 × 10^2 cells mL^{-1} (SAS2B) to
335 4.6 × 10^5 cells mL^{-1} (KWK1), equivalent to biovolume concentrations of 5.6 × 10^2 (SAS2B) to
336 1.9 × 10^6 μm^3 mL^{-1} (KWK1). In general, the lakes located on clays (KWK and BGR) contained
337 the highest cell concentrations and biovolume of total picophytoplankton. The shallow rock-
338 basin (SRB) and peatland lakes (SAS) were apparently less favourable, with picocyanobacterial
339 and picoeukaryote biovolume concentrations below 10^4 μm^3 mL^{-1}. Picoeukaryotes were
340 generally less numerically abundant than picocyanobacteria, but because of their larger cell size,
341 they often dominated the total picophytoplankton biomass. Picoeukaryotes accounted on average
342 (±SD) for 65 (±28) % of total picophytoplankton biovolume, however there was a wide range
343 among lakes in this contribution, from 8% (SAS2B) to 99% (SAS1A).
344
345 Total picophytoplankton biovolume increased with Chl *a* concentration (R = 0.52; p = 0.03),
346 but this relationship was only significant for the eukaryotic component (R = 0.53; p = 0.02).
347 Picocyanobacteria correlated negatively with DOC (R = -0.47; p = 0.05), while picoeukaryotes
348 correlated negatively with conductivity (R = -0.48; p = 0.05). Picocyanobacteria were highly
349 correlated with zeaxanthin (R = 0.72; p = 0.0002), and there was also a significant, albeit less
350 strong, correlation between picoeukaryotes and zeaxanthin (R = 0.54; p = 0.02). Stepwise
351 multiple linear regression models showed that picophytoplankton (picoeukaryotes, PEuk;
352 picocyanobacteria, PCyan) biovolumes were statistically related to certain limnological variables

353 according to the relationships: PEuk = 14.9 + 2.9 × Chl *a* - 1.7 × TN (R^2 = 0.56, p = 0.001), and
354 PCyan = -2.9 + 4.3 Temp + 1.1 × Chl *a* - 1.1 × TSS + 1.5 × TP - 1.2 × DOC (R^2 = 0.67,
355 p = 0.001).
356
357 **3.4 Molecular analyses**
358 The 18S rRNA data set from the palsa thaw lake (SAS2A) contained large numbers of rotifer
359 sequences (400 to 1350 reads per sample, all with closest matches to the genus *Ascomorpha*) and
360 these were removed prior to further analysis. This left a total of 3857 and 3128 reads for the
361 surface L (> 3.0 µm) and S (< 3.0 µm) fractions, and 3522 and 2457 reads for the bottom L and S
362 fractions; 84 to 93% of these eukaryotic sequences could be assigned (≥ 98% identity) to phylum
363 in the modified SILVA database. The largest fraction of total reads was attributable to ciliates
364 (up to 33% in the surface waters and 74% in the bottom waters; Table 4), including the genus
365 *Stokesia,* especially in the surface waters, and the genera *Cryptocaryon, Halteria*, *Peniculida* and
366 *Cyclidium*, especially in the bottom waters (Table 5). Among the groups nominally considered as
367 phytoplankton were dinoflagellates, chrysophytes and chlorophytes, with lesser proportions of
368 reads associated with katablepharids, bacillariophytes (diatoms) and cryptophytes (Table 4).
369 Analysis of the dissimilarity distances (Bray-Curtis distance on the sub-sampled dataset) showed
370 that community structure greatly differed with depth (Bray-Curtis dissimilarity index of 0.795
371 for the large fraction and 0.820 for the small fraction), and to a much lesser extent between large
372 and small fractions (Bray-Curtis dissimilarity index of 0.423 for the surface samples and 0.312
373 for the bottom samples). Chlorophytes, dinoflagellates, katablepharids and diatoms were more
374 represented in the large, surface water fraction.
375

4 Discussion

Each of the subarctic thaw lakes contained pigments from several phytoplankton phyla, revealing that these abundant waters provide habitats for diverse phototrophic groups., The most abundant accessory pigment (apart from β,β-carotene present in all algal groups) was fucoxanthin, indicating the possible presence of diatoms, chrysophytes or certain dinoflagellates. Peridinin and alloxanthin were also present in many of the samples, indicating the presence of dinoflagellates and cryptophytes, respectively (Jeffrey et al., 2011). Diatoms would be less favoured in these stratified waters given their relatively high sinking rates, while flagellated taxa including chrysophytes, dinoflagellates and cryptophytes would be able to maintain their position in the euphotic zone. Mixotrophic chrysophytes and dinoflagellates have been observed in many high latitude lakes (Charvet et al., 2012; and references therein), and may be additionally favored by the high biomass concentrations of heterotrophic bacteria that occur in some of these waters (Breton et al., 2009; Roiha et al., 2015). Green algae were also well represented at most sites, indicating that despite the strong light attenuation by CDOM and TSS (Watanabe et al., 2011), there is adequate light availability for obligate phototrophs. Another conspicuous feature of the pigment data was the large variation in pigment characteristics among lakes within the same valley, even between adjacent waterbodies. This large within-valley variation has also been observed in bacterial studies in the region (Crevecoeur et al., 2015; Comte et al., 2015).

The concentrations of photoprotective pigments were conspicuously high in NASH relative to photosynthetic pigments (Table 2). This was unexpected given that it contained elevated concentrations of suspended solids, which indicate a low light availability for photosynthesis, and a lack of need for protection against bright light. It is possible, however, that in this lake,

399 cells suspended in the mixed layer are adapted to intermittent exposure to bright light rather than
400 the average water column irradiance. Such conditions have been observed in a turbid estuarine
401 environment, where the phytoplankton were photosynthetically adapted to high near-surface
402 irradiances rather than the overall shade or dark conditions experienced on average by the cells
403 as they were circulated by turbulent mixing through the water column (Vincent et al., 1994). In
404 contrast, the ratio of photosynthetic to photoprotective pigments was high in NASA and the SAS
405 lakes, indicating acclimation to low irradiances in their strongly light-attenuating water columns.
406
407 The pigment analyses also indicated the abundant presence of cyanobacteria. Echinenone and
408 canthaxanthin are well known photoprotective pigments in cyanobacteria, with the latter
409 especially prevalent in Nostocales, which may suggest the presence of nitrogen-fixing taxa.
410 These results are consistent with bacterial 16S rRNA analyses, which showed the presence of
411 cyanobacterial taxa in some of these lakes that had strong affinities (> 99% sequence similarity)
412 to the Nostocalean taxon *Dolichospermum curvum* (Crevecoeur et al., 2015). Zeaxanthin can
413 potentially occur in high cellular concentrations in cyanobacteria, but it also is found in
414 eukaryotic algal groups. This pigment is a component of photoprotective xanthophyll cycles, and
415 may co-occur with other components of these cycles. For example, studies on the diatom
416 *Phaedactylum tricornutum* have shown the co-occurrence of the diadinoxanthin cycle and the
417 violaxanthin cycle (Lohr and Wilhelm, 1999). Consistent with this co-occurrence, we found a
418 strong correlation between diadinoxathin and violaxanthin in the studied lakes ($R = 0.72$,
419 $p < 0.001$). We also observed high concentrations of zeaxanthin, which is often associated with
420 cyanobacteria but also chlorophytes (Jeffrey et al., 2011). Given the molecular analyses results of
421 thaw lake bacterial communities (Crevecoeur et al., 2015) and our flow cytometry data,

zeaxanthin was likely to be at least in part associated with the abundant picocyanobacteria in the order Synechococcales. The strong correlation between picocyanobacteria and zeaxanthin further supports this relationship.

HPLC analysis has been used with success in a variety of aquatic ecosystems to not only identify major algal groups, but also to quantify their proportional representation using the software program CHEMTAX (Mackay et al., 1996). However, given the large known variation in pigment ratios in algal cells, this method requires extensive calibration on each class of waters. For example, in shallow a eutrophic lake, CHEMTAX gave a reliable estimation of cyanobacterial and chlorophyte biomass, but not chrysophytes and dinoflagellates (Tamm et al., 2015). The latter were two of the dominant groups in the permafrost thaw lakes, and although CHEMTAX offers a potentially useful approach for future analyses of these waters, further work will be required before it can be calibrated and reliably applied.

The presence of bacteriochlorophyll *d* in high concentrations in KWK lakes containing anoxic bottom waters indicate that these environments are favourable habitats for photosynthetic sulfur bacteria. These results were unexpected given the strong attenuation of light by the CDOM and suspended particles in these waters, and the low photosynthetically available radiation at depth. However, the results are consistent with molecular analyses of the bacterial assemblages. 16S rRNA gene clone library analysis of KWK lakes detected the presence of green sulfur bacteria (Rossi et al., 2013), and high throughput 16S rRNA sequencing revealed that the green sulfur bacterium *Pelodictyon* (Chlorobi) was one of the most abundant sequences in KWK waters (Crevecoeur et al., 2015). The high concentrations of bacteriochlorophyll *d* suggest that these

445 populations could play an important role in the overall primary production of certain thaw lakes,
446 albeit restricted to anoxic conditions well below the surface, and our observations extend the
447 range of environments in which this pigment has been detected.
448
449 Picophytoplankton occurred in all of the sampled lakes, but with large differences among waters
450 in terms of the relative abundance of prokaryotes versus eukaryotes, and probably also in terms
451 of their contribution to the total phytoplankton community biomass. As a first estimate of the
452 relative contribution of picocyanobacteria, their cell concentrations may be converted to
453 equivalent Chl *a* by an appropriate cell conversion factor. Analysis of *Synechococcus* in culture
454 under different irradiance regimes gave a median value around 7.5 fg Chl *a* per cell (Moore et al.
455 1995), and applying this value as a first order estimate, picocyanobacteria would contribute 0.3%
456 (SAS1B) to 80% (KWK23) of the measured total community Chl *a*. Such estimates are highly
457 approximate given the known variation in the cellular content of this pigment among strains and
458 with growth conditions; for example, by a factor of 4 as a function of irradiance (Moore et al.
459 1995). However these calculations imply large lake-to-lake variations in the percentage
460 contribution of picophytoplankton to the total community, ranging from negligible to major.
461
462 In general, the concentrations of both picocyanobacteria and picoeukaryotes increased with
463 increasing total phytoplankton biomass, as measured by Chl *a* concentrations. However, the two
464 groups differed in their correlative relationships with other limnological variables. In partial
465 support of our initial hypothesis that DOC would be a controlling variable, picocyanobacteria,
466 but not eukaryotes, were negatively correlated with DOC. An inverse relationship with DOC was
467 also found for picophytoplankton in Swedish lakes (Drakare et al., 2003). Similarly in Lake

Valkea-Kotinen, in the boreal zone of Finland, variations in autotrophic picoplankton were most closely correlated with water column stability, which in turn was strongly regulated by DOC concentration (Peltomaa and Ojala, 2012). High DOC waters are often characterized by low pH, which may be a constraint on certain cyanobacteria, however acid-tolerant picocyanobacteria are known (Jasser et al., 2013). Even in the low pH SAS waters picocyanobacteria were always present, although in low concentrations (e.g., the minimum of 1.8×10^3 mL^{-1} in SAS2B in 2011). Other factors such as zooplankton grazing may also have played a role in controlling picocyanobacteria (Rautio and Vincent, 2006), although this seems less likely for picocyanobacteria given that they are a nutritionally deficient food source for zooplankton in thaw lakes (Przytulska et al., 2015).

Picocyanobacteria did not show the expected relationship with temperature in the correlation analyses, although temperature was one of the variables retained in the multiple linear regression analysis. Temperature has often been identified as a key variable for cyanobacterial growth and dominance in lakes elsewhere. For example, in reservoirs in the southeastern USA, there was a strong, positive correlation between picocyanobacterial cell concentrations and temperature, while picoeukaryotes showed an inverse correlation, and dominance of the picophytoplankton community shifted from picoeukaryotes in winter to picocyanobacteria in summer (Ochs and Rhew, 1997). Similarly, increasing temperature favoured picocyanobacteria over picoeukaryotes in German lakes (Hepperle and Krienitz, 2001). In experiments with subarctic lake and river water at 10 and 20°C, the concentration of Chl *a* in the picoplankton fraction increased substantially at the warmer temperature (Rae and Vincent, 1998). The temperature range in the present study may have been too restricted to observe such effects.

The molecular data provided insight into the large diversity of microbial eukaryotes that occur within the plankton of thaw lake ecosystems, including heterotrophic components such as ciliates and flagellates that may exert grazing pressure on some of the phototrophs. When rotifers were excluded from the analyses, ciliates were dominant in the RNA sequences of SAS2A. This likely reflects not only their cellular abundance but also their large cell sizes with a concomitantly large number of ribosomes; for example, *Stokesia vernalis,* the most abundant sequence identified in the surface waters (Table 5), can be >100 µm in length. Ciliates are also known to be fragile cells that are easily broken up during manipulation like pre-filtration through a 20 µm mesh, which could account for their highly abundant sequences in the S as well as L fractions.

Chrysophytes and chlorophytes were well represented in the RNA sequences, particularly in the surface water L fraction, consistent with their abundance as indicated by the pigment data. Dinoflagellates constituted the dominant fraction of the phytoplankton sequences, yet were not detected as peridinin in SAS2A, although this pigment was present in two other SAS lakes. This may indicate the presence of large dinoflagellate cells, for example rigid *Ceratium* cells that can extend up to 100 µm in length, but may also be due to the presence of dinoflagellates that lack the accessory pigment peridinin. It should also be noted that the relative abundance of taxa in these analyses may additionally reflect PCR biases in amplification (Potvin and Lovejoy, 2009). Diatoms can also include large cell types, but their representation in the sequences was small, suggesting that most of the fucoxanthin that we measured was associated with chrysophytes such as *Uroglena* (Table 5) rather than diatoms. It is of interest that diatoms from the genus *Urosolenia* were the closest match following a BLAST search. This diatom is known to be

514 lightly silicified and may be less susceptible to sedimentation in these well stratified waters. The
515 cryptophyte pigment alloxanthin was in high concentration in SAS2A, as in the other thaw lakes,
516 yet cryptophyte sequences accounted for < 1.5% of the total RNA reads. This might reflect the
517 small cell-size of certain cryptophyte taxa, for example *Chroomonas*.
518
519 The molecular data also provided insight into the nature of the picoeukaryotic communities in
520 the SAS lakes. The taxonomic identities (Table 5) indicated the presence of several chlorophyte
521 genera that are known to produce small cells, notably *Choricystis*, *Lemmermannia*
522 *Monoraphidium* and *Chlorella*. For example, in subalpine Lake Tahoe (USA), *Choricystis*
523 *coccoides* produces cells that are only 0.5 μm^3 in volume, too small to be grazed by calanoid
524 copepods in that lake (Vincent, 1982). Among the chrysophytes, *Spumella* and related genera are
525 known to produce small cells. For all of these analyses, the many unidentified eukaryotic reads
526 add an extra element of uncertainty to the interpretation, but collectively these data underscore
527 the eukaryotic diversity of the thaw lake ecosystem. This parallels the large prokaryotic diversity
528 that has been observed in these lakes, including bacterial phototrophs (Crevecoeur et al., 2015;
529 Comte et al., 2015).
530
531 Permafrost thaw lakes receive large quantities of allochthonous organic carbon from their
532 surrounding catchments and this is reflected in their high DOC and CDOM concentrations, as
533 observed in the present study. These waters have high respiratory oxygen demands and are net
534 heterotrophic, resulting in prolonged hypoxia or anoxia in the bottom waters during summer, and
535 anoxia throughout the water column once ice covers the lake in winter (Deshpande et al., 2015).
536 The abundant ciliate and nanoflagellate sequences in our molecular analyses also point to high

productivity by bacterial heterotrophs, their likely prey in these waters. However, despite these multiple signs of intense heterotrophy, the pigment, cytometry and molecular results in the present study show that these ecosystems are also the habitats for abundant phototrophs from diverse taxonomic groups.

Conclusions

The wide range of thaw lakes sampled in the present study significantly differed from the reference rock basin lakes in their limnological properties. On average, they contained higher phytoplankton (Chl *a*) and TP concentrations than the reference lakes, but had a comparable diversity of pigments, dominated by chlorophyte, chrysophyte and dinoflagellate pigments. Cyanobacteria and cryptophytes were also well represented, but the thaw waters appeared to be less favorable for diatoms, at least during the highly stratified late-summer period. Picophytoplankton occurred in all of the thaw lakes, in some of the waters at high biovolume up to 10^6 μm^3 mL^{-1}, but the proportion of eukaryotes and prokaryotes and their contribution to total phytoplankton biomass varied greatly among the lakes. Molecular analysis of samples from one thaw lake in the degraded permafrost, peatland valley indicated that small cell chlorophytes may be among the dominants in the picoeukaryotic fraction. Despite the heterotrophic nature of these organic-rich ecosystems, with respiration likely exceeding photosynthesis throughout the year, permafrost thaw lakes contain abundant, diverse phototrophs that potentially support higher trophic levels, and that will lessen the net CO_2 release from these waters to the atmosphere.

Author contributions

A. P., W. F. V. and I. L. designed the study; A. P. led the field sampling; S. C. with input from J. C. undertook the molecular analyses under the supervision of C. L.; laboratory analyses were overseen by A. P., W. F. V. and I. L.; flow cytometry analyses were by J. C. and A. P., under the supervision of I. L.; and data analysis was by A. P. with input from J. C., S. C. and W. F. V. A. P. prepared the manuscript with contributions from all co-authors.

Acknowledgments

We thank Marie-Josée Martineau for laboratory assistance with the HPLC analyses, and ADAPT colleagues Paschale Bégin, Bethany Deshpande and Alex Matveev, for assistance in the field. We are also grateful to Maciej Bartosiewicz for his help throughout this project, Adam Monier for bioinformatics advice, and Sylvia Bonilla, Ladd Johnson and two anonymous referees for their insightful comments on the manuscript. This study was funded by the Natural Sciences and Engineering Research Council of Canada (NSERC) including the Discovery Frontiers ADAPT grant to W. F. V., an EnviroNord fellowship to J. C., Fonds de recherche du Québec, the Network of Centres of Excellence ArcticNet and the Canada Research Chair program.

References

Alexander, V., Stanley, D. W., Daley, R. J. and McRoy, C. P.: Primary producers, in: Hobbie, J. E. (Ed.) Limnology of Tundra Ponds, Barrow, Alaska, Dowden, Hutchinson and Ross Inc., Stroudsburg, PA, U.S./IBP Synthesis Series, 13, 179–250, 1980.

Ansotegui, A., Trigueros, J. M., and Orive, E.: The use of pigment signatures to assess phytoplankton assemblage structure in estuarine waters, Estuar. Coast. Shelf Sci., 52, 689–703, 2001.

Benjamini, Y., and Hochberg, Y.: Controlling the false discovery rate: a practical and powerful approach to multiple testing, J. Roy. Stat. Soc., Series B, 57, 289–300, 1995.

Bergeron, M., and Vincent, W. F.: Microbial food web responses to phosphorus and solar UV radiation in a subarctic lake, Aquat. Microb. Ecol., 12, 239–249, 1997.

Bhiry, N., Delwaide, A., Allard, M., Bégin, Y., Filion, L., Lavoie, M., Payette, S., Pienitz, R., Nozais, C., Saulnier-Talbot, É., and Vincent, W. F.: Environmental change in the Great Whale River region, Hudson Bay: Five decades of multidisciplinary research by Centre d'études nordiques (CEN), Ecoscience, 18, 182–203, doi:10.2980/18-3-3469, 2011.

Bonilla, S., Villeneuve, V., and Vincent, W. F.: Benthic and planktonic algal communities in a high arctic lake: pigment structure and contrasting responses to nutrient enrichment, J. Phycol., 41, 1120–1130, doi:10.1111/j.1529-8817.2005.00154.x, 2005.

Bouchard, F., Pienitz, R., Ortiz, J. D., Francus, P., and Laurion, I.: Palaeolimnological conditions inferred from fossil diatom assemblages and derivative spectral properties of sediments in thermokarst ponds of subarctic Quebec, Canada, Boreas 42, 575–595, doi:10.1111/bor.12000, 2013.

Breton, J., Vallières, C., and Laurion, I.: Limnological properties of permafrost thaw ponds in northeastern Canada, Can. J. Fish. Aquat. Sci., 66, 1635–1648, doi:10.1139/F09-108, 2009.

Caplanne, S., and Laurion, I.: Effects of chromophoric dissolved organic matter on epilimnetic stratification in lakes, Aquat. Sci., 70, 123–133, doi:10.1007/s00027-007-7006-0, 2008.

Caporaso, J. G., Kuczynski, J., Stombaugh, J., Bittinger, K., Bushman, F. D., Costello, E. K., and Fierer, N.: QIIME allows analysis of high-throughput community sequencing data, Nature Methods, 7, 335–336, doi:10.1038/nmeth.f.303.QIIME, 2010.

Charvet, S., Vincent, W. F., and Lovejoy, C.: Chrysophytes and other protists in high Arctic lakes: molecular gene surveys, pigment signatures and microscopy, Polar Biol., 35, 733–748, doi:10.1007/s00300-011-1118-7, 2012.

Comeau, A. M., Li, W. K. W., Tremblay, J.-É., Carmack, E. C., and Lovejoy, C.: Arctic Ocean microbial community structure before and after the 2007 record sea ice minimum, PloS ONE, 6, e27492, doi:10.1371/journal.pone.0027492, 2011.

610 Comte, J., Monier, A., Crevecoeur, S. M., Lovejoy, C., and Vincent, W. F.: Bacterial
611 biogeography of permafrost thaw lakes in the changing northern landscape, Ecography, 38,
612 doi: 10.1111/ecog.01667, 2015.

613 Crevecoeur, S., Vincent, W. F., Comte, J., and Lovejoy, C.: Bacterial community structure
614 across environmental gradients in permafrost thaw ponds: Methanotroph-rich ecosystems,
615 Front. Microbiol., 6, 192, doi:10.3389/fmicb.2015.00192, 2015.

616 Deshpande, B. N., MacIntyre S., Matveev A., and Vincent, W. F.: Oxygen dynamics in
617 permafrost thaw lakes: Anaerobic bioreactors in the Canadian subarctic. Limnol. Oceanogr.,
618 60, 1656-1670, doi:10.1002/lno.10126, 2015.

619 Drakare, S., Blomqvist, P., Bergström, A. K., and Jansson, M.: Relationships between
620 picophytoplankton and environmental variables in lakes along a gradient of water colour and
621 nutrient content, Freshwat. Biol., 48, 729–740, doi:10.1046/j.1365-2427.2003.01049.x, 2003.

622 Edgar, R. C.: UPARSE: highly accurate OTU sequences from microbial amplicon reads, Nature
623 Methods, 10, 996–998, doi:10.1038/nmeth.2604, 2013.

624 Fietz, S., and Nicklisch, A.: An HPLC analysis of the summer phytoplankton assemblage in
625 Lake Baikal, Freshwater Biol., 49, 332–345, doi: 10.1111/j.1365-2427.2004.01183.x, 2004.

626 Hepperle, D., and Krienitz, L.: Systematics and ecology of chlorophyte picoplankton in German
627 inland waters along a nutrient gradient, Int. Rev. Hydrobiol., 86, 269–284, 2001.

628 Jasser, I., Karnkowska-Ishikawa, A., and Chróst, R. J.: Do acid-tolerant picocyanobacteria exist?
629 A study of two strains isolated from humic lakes in Poland, Hydrobiologia, 707, 209–218,
630 doi:10.1007/s10750-012-1428-y, 2013.

631 Jeffrey, S. W., Wright, S. W., and Zapata, M.: Microalgal classes and their signature pigments,
632 in: Roy, S., Llewellyn, C. A., Skarstad Egeland, E., and Johnsen, G. (Eds) Phytoplankton
633 Pigments: Characterization, Chemotaxonomy and Applications in Oceanography, Cambridge
634 University Press. (SCOR), 52–53, 2011.

635 Jones, M., Grosse, G., Jones, B. M., and Walter Anthony, K. M.: Peat accumulation in a
636 thermokarst-affected landscape in continuous ice-rich permafrost, Seward Peninsula, Alaska,
637 J. Geophys. Res., 117, G00M07, doi:10.1029/2011JG001766, 2012.

638 Laurion, I., Vincent, W. F., MacIntyre, S., Retamal, L., Dupont, C., Francus, P., and Pienitz, R.:
639 Variability in greenhouse gas emissions from permafrost thaw ponds, Limnol. Oceanogr., 55,
640 115–133, doi:10.4319/lo.2010.55.1.0115, 2010.

641 Legendre, P., and Legendre, L.: Numerical Ecology, 3rd English Edition, Elsevier, 2012.

642 Lohr, M., and Wilhelm, C.: Algae displaying the diadinoxanthin cycle also possess the
643 violaxanthin cycle, Proc. Natl. Acad. Sci. U.S.A., 96, 8784–8789, 1999.

644 Lovejoy, C., Comeau, A., and Thaler, M.: Curated reference database of SSU rRNA for northern
645 marine and freshwater communities of Archaea, Bacteria and microbial eukaryotes, v. 1.0.
646 Nordicana D, in press, 2015.

647 Mackey, M. D., Mackey, D. J., Higgins, H. W., and Wright, S. W.: CHEMTAX—a program for
648 estimating class abundances from chemical markers: application to HPLC measurements of
649 phytoplankton, Mar. Ecol. Prog. Ser., 144, 265–83, doi:10.3354/meps144265, 1996.

650 Moore, L. R., Goericke, R., and Chisholm, S. W.: Comparative physiology of *Synechococcus*
651 and *Prochlorococcus* - influence of light and temperature on growth, pigments, fluorescence
652 and absorptive properties, Mar. Ecol.-Progr. Ser., 116, 259–275, 1995.

653 Ochs, C. A., and Rhew, K.: Population dynamics of autotrophic picoplankton in a southeastern
654 U.S. reservoir, Int. Rev. Hydrobiol. Hydrogr., 82, 293–313, 1997.

655 Oksanen, J., Blanchet, G. F., Kindt, R., Legendre, P., Minchin, P. R., O'Hara, R. B., Simpson, G.
656 L., Solymos, P., Henry, M., Stevens, H., and Wagner H.: Vegan: Community Ecology
657 Package, R package version 2.2-1, http://CRAN.R-project.org/package=vegan, 2015.

658 Paterson, A. M., Keller, W., Rühland K. M., Jones C. F., and Winter J. G.: An exploratory
659 survey of summer water chemistry and plankton communities in lakes near the Sutton river,
660 Hudson Bay lowlands, Ontario, Canada, Arct. Antarct. Alp. Res., 46, 121–138,
661 doi:10.1657/1938-4246-46.1.121, 2014.

662 Peltomaa, E., and Ojala, A.: Meteorological drivers of the dynamics of autotrophic picoplankton,
663 Freshwat. Biol., 57, 1005–1016, doi:10.1111/j.1365-2427.2012.02761.x, 2012.

664 Paerl, H. W., and Huisman, J.: Blooms like it hot, Science, 320, 57–58,
665 doi:10.1126/science.1155398, 2008.

666 Pienitz, R., Doran, P. T., and Lamoureux S. F.: Origin and geomorphology of lakes in the polar
667 regions, in: Polar Lakes and Rivers - Limnology of Arctic and Antarctic Aquatic Ecosystems,
668 Oxford University Press, Oxford, U.K., 25–41, 2008.

669 Potvin M., and Lovejoy C.: PCR-based diversity estimates of artificial and environmental 18S
670 rRNA gene libraries. J. Eukaryot. Microbiol., 56, 174–181, doi:10.1111/j.1550-
671 7408.2008.00386.x, 2009.

672 Pruesse, E., Quast, C., Knittel, K., Fuchs, B. M., Ludwig, W., Peplies, J., and Glockner, F. O.:
673 SILVA: a comprehensive online resource for quality checked and aligned ribosomal RNA
674 sequence data compatible with ARB, Nucleic Acids Res., 35, 7188–7196,
675 doi:10.1093/nar/gkm864, 2007.

676 Przytulska, A., Bartosiewicz, M., Rautio, M., Dufresne, F., and Vincent, W. F.: Climate effects
677 on high latitude *Daphnia* via food quality and thresholds, PLoS ONE, 10, e0126231,
678 doi:10.1371/journal.pone.0126231, 2015.

679 R Core Team: R: A Language and Environment for Statistical Computing, R Foundation for
680 Statistical Computing, Vienna, Austria, http://www.R-project.org/, 2014.

681 Rae, R. and Vincent, W. F.: Effects of temperature and ultraviolet radiation on microbial
682 foodweb structure: potential responses to global change, Freshwat. Biol., 40, 747–758,
683 doi:10.1046/j.1365-2427.1998.00361.x, 1998.

684 Rautio, M., and Vincent, W. F.: Benthic and pelagic food resources for zooplankton in shallow
685 high latitude lakes and ponds, Freshwat. Biol., 51, 1038–1052, doi:10.1111/j.1365-
686 2427.2006.01550.x, 2006.

687 Richardson, T. L., and Jackson, G. A.: Small phytoplankton and carbon export from the surface
688 ocean, Science, 315(5813), 838–840, doi:10.1126/science.1133471, 2007.

689 Roiha, T., Rautio, M., and Laurion I.: Carbon dynamics in highly net heterotrophic subarctic
690 thaw ponds, Biogeosci., in press, 2015

691 Rossi P., Laurion I., and Lovejoy C.: Distribution and identity of bacteria in subarctic permafrost
692 thaw ponds, Aquat. Microb. Ecol., 69, 231–245, doi:10.3354/ame01634, 2013.

693 Roy, S., Llewellyn, C. A., Egeland, E. S., and Johnsen, G. (Eds.): Phytoplankton Pigments:
694 Characterization, Chemotaxonomy and Applications in Oceanography, Cambridge University
695 Press., United Kingdom, 845 pp, 2011.

696 Schloss, P. D., Westcott, S. L., Ryabin, T., Hall, J. R., and Hartmann, M.: Introducing mothur:
697 Open-source, platform-independent, community-supported software for describing and
698 comparing microbial communities. Appl. Environ. Microbiol., 75, 7537–7541,
699 doi:10.1128/AEM.01541-09, 2009.

700 Stainton, M., Capel, M., and Armstrong, F.: The Chemical Analysis of Fresh Water, 2nd ed.,
701 Special Publication 25, Canada Fisheries and Marine Service, 1977.

702 Tamm, M., Freiberg, R., Tõnno, I., Nõges, P., and Nõges ,T.: Pigment-based chemotaxonomy - a
703 quick alternative to determine algal assemblages in large shallow eutrophic lake?, PLoS ONE,
704 10, e0122526, doi:10.1371/journal.pone.0122526, 2015.

705 Vallières, C., Retamal, L., Ramlal, P., Osburn, C. L., and Vincent, W. F.: Bacterial production
706 and microbial food web structure in a large arctic river and the coastal Arctic Ocean, J.
707 Marine Syst., 74, 756–773, doi:10.1016/j.jmarsys.2007.12.002, 2008.

708 Van Hove, P., Vincent, W. F., Galand, P. E., and Wilmotte, A.: Abundance and diversity of
709 picocyanobacteria in high arctic lakes and fjords, Algological Studies, 126, 209–227,
710 doi:10.1127/1864-1318/2008/0126-0209, 2008.

711 Vincent, W. F.: The autecology of an ultraplanktonic shade alga in Lake Tahoe, J. Phycol., 18,
712 226–232, 1982.

713 Vincent, W.F., Bertrand, N., and Frenette, J-J.: Photoadaptation to intermittent light across the
714 St. Lawrence Estuary freshwater-saltwater transition zone, Mar. Ecol.-Prog. Ser., 110, 283–
715 292, 1994.

716 Waleron, M., Waleron, K., Vincent, W. F., and Wilmotte, A.: Allochthonous inputs of riverine
717 picocyanobacteria to coastal waters in the Arctic Ocean, FEMS Microbiol. Ecol., 59, 356–
718 365, doi:10.1111/j.1574-6941.2006.00236.x, 2007.

719 Walter, K. M., Zimov, S.A., Chanton, J. P., Verbyla, D., and Chapin, F. S. III: Methane bubbling
720 from Siberian thaw lakes as a positive feedback to climate warming, Nature, 443, 71–75,
721 doi:10.1038/nature05040, 2006.

722 Watanabe, S., Laurion, I., Chokmani, K., Pienitz, R., and Vincent, W. F.: Optical diversity of
723 thaw ponds in discontinuous permafrost: A model system for water color analysis, J.
724 Geophys. Res.-Biogeo., 116, G02003, doi:10.1029/2010JG001380, 2011.

725

Table 1. Limnological characteristics including surface values for temperature (T), pH, dissolved organic carbon concentration (DOC), colored dissolved organic matter (CDOM), total suspended solids (TSS), soluble reactive phosphorus (SRP), total phosphorus (TP), total nitrogen (TN), nitrate (NO_3) and Chlorophyll *a* (Chl *a*) in studied subarctic lakes. Mean values from 2011 and 2012 (± range in brackets; nd = no data from 2011).

Sites	T (°C)	pH	DOC (mg L^{-1})	CDOM (m^{-1})	TSS (mg L^{-1})	SRP (µg L^{-1})	TP (µg L^{-1})	TN (mg L^{-1})	NO_3 (mg N L^{-1})	Chl *a* (µg L^{-1})
Thaw lakes on northern clay soils										
BGR1	15.1 (0.7)	7.5 (0.2)	3.9 (0.4)	6.1 (1.7)	2.9 (0.5)	1.8 (0.6)	17.3 (3.5)	0.1 (0.0)	0.05 (0.0)	1.8 (1.0)
BGR2	14.5 (0.4)	7.0 (0.3)	9.0 (0.3)	39.1 (5.7)	19.2 (6.1)	2.4 (1.0)	45.7 (0.2)	0.3 (0.0)	0.05 (0.0)	3.4 (1.4)
NASA	15.6 (nd)	7.0 (nd)	3.0 (nd)	12.3 (nd)	319.3 (nd)	2.9 (nd)	124.5 (nd)	3.7 (nd)	0.25 (nd)	4.1 (nd)
NASH	18.3 (nd)	7.6 (nd)	4.1 (nd)	22.6 (nd)	18.2 (nd)	6.2 (nd)	28.5 (nd)	0.4 (nd)	0.04 (nd)	1.7 (nd)
Thaw lakes on southern clay soils										
KWK1	17.1 (4.4)	6.1 (0.8)	9.2 (2.8)	39.0 (16.4)	14.1 (12.0)	2.2 (1.5)	36.8 (26.7)	0.3 (0.1)	0.05 (0.0)	8.0 (1.2)
KWK6	14.9 (0.8)	6.8 (0.4)	5.2 (0.0)	10.7 (0.7)	9.3 (1.1)	1.0 (0.4)	30.9 (3.0)	0.2 (0.0)	0.06 (0.0)	4.4 (1.6)
KWK12	16.8 (0.8)	8.0 (1.1)	8.6 (0.7)	39.6 (3.7)	13.8 (2.6)	1.6 (0.0)	27.7 (2.1)	0.2 (0.0)	0.08 (0.0)	2.5 (0.1)
KWK23	14.9 (0.2)	6.7 (0.2)	7.2 (0.6)	35.8 (1.9)	10.2 (1.9)	4.9 (0.6)	47.7 (5.6)	0.2 (0.0)	0.04 (0.0)	3.5 (1.9)
Thaw lakes on peatlands										
SAS1A	14.3 (0.2)	6.6 (0.3)	10.7 (0.8)	68.7 (2.7)	7.6 (2.6)	1.6 (0.3)	14.3 (0.9)	0.5 (0.1)	0.17 (0.0)	3.6 (1.2)
SAS1B	13.6 (0.1)	6.3 (0.3)	15.9 (0.4)	109.5 (3.9)	21.8 (5.4)	1.9 (0.4)	12.7 (2.2)	0.6 (0.1)	0.07 (0.0)	4.3 (0.1)
SAS2A	19.9 (nd)	6.2 (nd)	14.9 (nd)	98.4 (nd)	2.6 (nd)	3.1 (nd)	9.6 (nd)	0.7 (nd)	0.04 (nd)	1.2 (nd)
SAS2B	16.0 (nd)	6.0 (nd)	17.1 (nd)	116.9 (nd)	5.2 (nd)	1.3 (nd)	10.3 (nd)	0.5 (nd)	0.11 (nd)	0.9 (nd)
Shallow rock-basin lakes										
SRB1	15.8 (2.2)	7.6 (0.6)	9.9 (0.0)	46.0 (6.5)	2.6 (1.2)	2.1 (0.6)	7.9 (2.8)	0.2 (0.1)	0.06 (0.0)	0.3 (0.1)
SRB2	13.8 (0.5)	7.6 (1.1)	13.2 (2.7)	68.8 (21.5)	1.3 (0.3)	1.4 (0.5)	11.2 (2.6)	0.2 (0.1)	0.14 (0.1)	1.4 (0.4)
SRB3	15.6 (0.2)	6.6 (0.2)	7.8 (1.4)	34.5 (9.5)	5.4 (2.0)	1.1 (0.1)	13.4 (2.8)	0.3 (0.1)	0.05 (0.0)	5.2 (0.6)
SRB4	15.0 (0.3)	7.9 (0.5)	10.4 (1.6)	20.0 (0.5)	5.0 (1.9)	0.8 (0.1)	5.7 (2.6)	0.8 (0.4)	0.44 (0.4)	2.4 (1.0)
SRB5	18.7 (1.8)	7.1 (0.9)	3.7 (0.1)	9.4 (2.7)	0.7 (0.1)	0.5 (0.2)	2.9 (1.3)	0.1 (0.0)	0.32 (0.2)	0.8 (0.0)

Table 2. The dominant photosynthetic and photoprotective accessory pigments (nmol L^{-1}), their sums (Σ) and ratio in each of the subarctic water bodies sampled in 2012.

Sites	Photosynthetic					Photoprotective							Ratio
	Allo	Chl b	Fuco	Perid	Σ	Cantha	Diadino	Echin	Lut	Viola	Zea	Σ	
Thaw lakes on northern clay soils													
BGR1	0.282	0.108	0.174	0.034	0.598	0.000	0.113	0.045	0.126	0.132	0.080	0.497	1.2
BGR2	0.053	0.159	0.611	0.343	1.167	0.073	0.483	0.088	0.372	0.442	0.677	2.134	0.5
NASA	2.078	0.401	0.101	0.000	2.580	0.000	0.000	0.000	0.745	0.308	0.000	1.053	2.4
NASH	0.161	0.204	0.740	0.000	1.106	0.184	0.464	0.208	0.208	0.568	1.692	3.324	0.3
Thaw lakes on southern clay soils													
KWK1	0.641	1.681	0.702	0.458	3.481	0.147	3.836	0.202	1.435	0.847	0.375	6.843	0.5
KWK6	0.248	0.760	0.429	0.075	1.513	0.093	0.398	0.000	1.335	0.771	0.561	3.158	0.5
KWK12	0.290	0.202	0.569	0.151	1.213	0.046	0.358	0.089	0.337	0.354	0.111	1.295	0.9
KWK23	0.281	0.236	0.499	0.057	1.073	0.046	0.443	0.026	0.644	0.450	0.688	2.296	0.5
Thaw lakes on peatlands													
SAS1A	0.498	0.130	1.080	0.110	1.817	0.083	0.291	0.000	0.161	0.366	0.092	0.993	1.8
SAS1B	1.066	0.271	1.484	0.363	3.184	0.044	0.435	0.000	0.294	0.420	0.083	1.275	2.5
SAS2A	0.342	0.054	0.199	0.000	0.594	0.000	0.047	0.000	0.047	0.000	0.000	0.093	6.4
SAS2B	0.606	0.163	0.502	0.000	1.271	0.036	0.049	0.045	0.220	0.171	0.000	0.521	2.4
Shallow rock-basin lakes													
SRB1	0.018	0.038	0.051	0.017	0.124	0.000	0.026	0.008	0.045	0.069	0.026	0.175	0.7
SRB2	0.196	0.220	0.360	0.040	0.816	0.037	0.078	0.057	0.229	0.183	0.062	0.646	1.3
SRB3	1.026	0.352	2.011	0.261	3.650	0.103	0.460	0.219	0.557	0.924	0.530	2.792	1.3
SRB4	0.094	0.203	0.557	0.050	0.905	0.016	0.159	0.080	0.333	0.340	0.101	1.028	0.9
SRB5	0.066	0.048	0.420	0.004	0.537	0.010	0.085	0.031	0.064	0.199	0.087	0.477	1.1

Key: Allo, alloxanthin; Chl *b*, chlorophyll *b*; Fuco, fucoxathin; Perid, peridinin; Cantha, canthaxanthin; Diadino, diadinoxanthin; Echin, echinenone; Lut, lutein; Viola, violaxanthin; Zea, zeaxanthin.

Table 3. The relative concentration of bacteriochlorophyll *d* (BChl *d*, μg L^{-1}) based on chromatogram peak area at 430 nm. The KWK thaw sites have been arranged from lowest to highest concentrations of pigment.

Lake	Date	Depth (m)	BChl *d* (μg L^{-1})
KWK6	4 Aug 2012	3.1	1.2
KWK6	21 Aug 2011	3.1	1.3
KWK23	4 Aug 2012	2.0	1.9
KWK12	3 Aug 2012	2.0	8.2
KWK12	19 Aug 2011	2.5	24.6
KWK1	19 Aug 2011	2.0	28.9
KWK23	4 Aug 2012	3.3	36.2
KWK23	21 Aug 2011	3.3	44.3
KWK1	3 Aug 2012	2.0	44.7
KWK12	3 Aug 2012	2.5	47.3

Table 4. RNA sequence analysis of eukaryotes in samples from permafrost thaw lake SAS2A, sampled in 2012. Each value is the % number of reads of the total for each sample (total number of reads minus rotifer sequences). The large fraction was retained on a 3 μm filter and the small fraction was on a 0.2 μm filter after passing through the 3 μm pre-filter.

Taxonomic group	Percentage of reads			
	Surface		Bottom	
	Large	Small	Large	Small
Phytoplankton groups				
Dinophyta	17.11	4.02	8.71	1.90
Chrysophyta[a]	14.47	14.81	9.07	3.60
Chlorophyta[b]	9.97	2.03	2.11	0.40
Cryptophyta	3.10	1.71	2.39	0.65
Katablepharidophyta	2.71	1.00	0.11	0.20
Bacillariophyta	2.47	0.44	0.96	0.45
Raphidophyceae	0.51	0.33	0.00	0.04
Pavlovales	0.44	0.19	0.18	0.04
Prymnesiales	0.15	0.03	0.06	0.00
Other groups				
Ciliophora	22.94	43.55	62.95	83.90
Cercozoa	6.17	12.37	2.50	1.22
Fungi[c]	1.47	0.61	0.32	0.04
Centroheliozoa	1.44	0.80	0.11	0.12
Choanoflagellida	1.32	3.12	0.23	0.20
Perkinsea	0.00	0.00	0.03	0.12
Unknown affinities	15.75	15.00	10.28	7.11

[a]includes Chrysophyceae, Synurophyceae and Bicosoecida
[b]includes Chlorophyceae and Trebouxiophyceae
[c]includes Chytridiomycota, Oomycota and Ascomycota

Table 5. Closest identity (ID) of eukaryotic RNA sequences from permafrost thaw lake SAS2A to GenBank sequences (following a BLASTn search), at the lowest taxonomic level identified.

GenBank Taxonomy	Accession number	Isolation source	% ID	Percentage of reads	
				Surface	Bottom
Phytoplankton groups					
Chrysophyta					
Uroglena sp.	EU024983	FU44-26	99	6.03	0.03
Paraphysomonas sp.	JQ967316	Freshwater	99	0.67	3.78
Dinobryon divergens	KJ579346	WO33_4	99	0.40	0.00
Spumella-like flagellate	AY651098	Lake Mondsee	99	0.03	0.76
Cryptophyta					
Cryptomonas tetrapyrenoidosa	KF907407	Deokam032610	99	1.71	0.87
Cryptomonas pyrenoidifera	KF907397	CNUCRY 166	99	0.33	0.00
Cryptomonas curvata	KF907377	CNUCRY 90	99	0.06	0.28
Dinophyta					
Dinophyceae sp.	GQ423577	Lake Baikal	99	1.31	0.58
Peridinium wierzejskii	KF446619	Baikal region	99	1.03	2.07
Gyrodiniellum shiwhaense	FR720082	Shiwha Bay	98	0.49	0.01
Bacillariophyta					
Urosolenia eriensis	HQ912577	Y98-8	98	1.22	0.58
Chlorophyta					
Lemmermannia punctata	JQ356704	SAG 25.81	99	1.07	0.08
Chlorella sp.	Y12816	OvS/Ger1	99	1.00	0.00
Choricystis sp.	AY195972	AS-29	99	0.89	0.11
Koliella longiseta	HE610126	SAG 470-1	99	0.72	0.04
Monoraphidium sp.	KP017571	LB59	99	0.39	0.00
Raphidophyta					
Gonyostomum semen	KP200894	Freshwater	100	0.23	0.02
Prymnesiales					
Chrysochromulina parva	EU024987	FU44-40	100	0.09	0.03
Other groups					
Ciliophora					
Stokesia vernalis	HM030738	Freshwater	99	8.65	0.04
Cryptocaryon sp.	JF317699	Drinking water	99	0.89	5.61
Peniculida sp.	GQ330632	Peat bog water	98	0.83	1.85
Halteria sp.	GU067995	Lake water	99	0.49	6.38
Cyclidium marinum	JQ956553	Marine coast	99	0.00	34.42
Rhizaria					
Cercozoa	AB771834	Lake Kusaki	99	3.83	0.28
Fungi					
Saprolegnia sp.	FJ794911	Lake (parasite)	99	0.11	0.00
Penicillium brevicompactum	KP981369	ATCC 16024	99	0.00	0.10

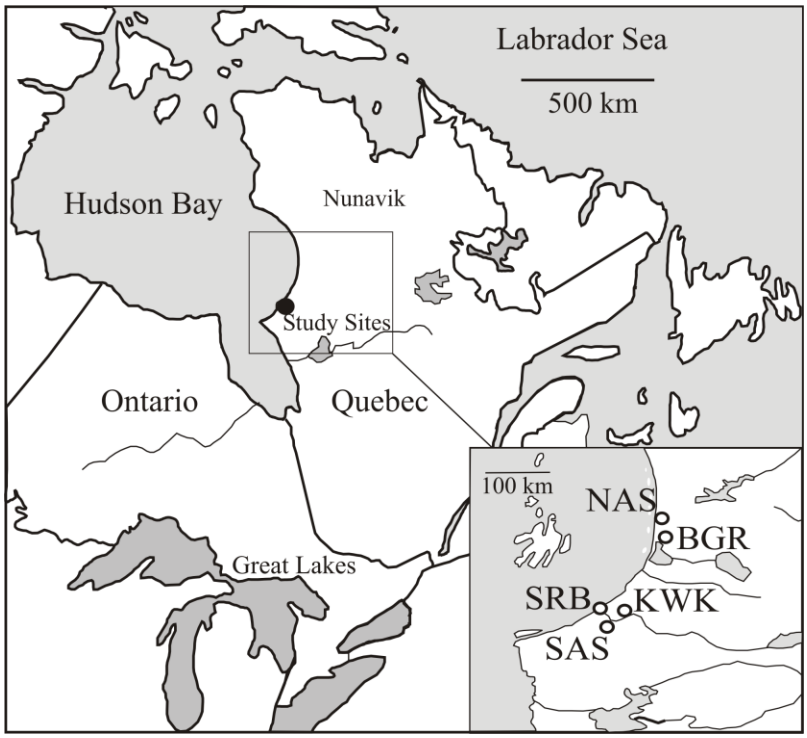

Figure 1. Location of the study area in Subarctic Quebec.

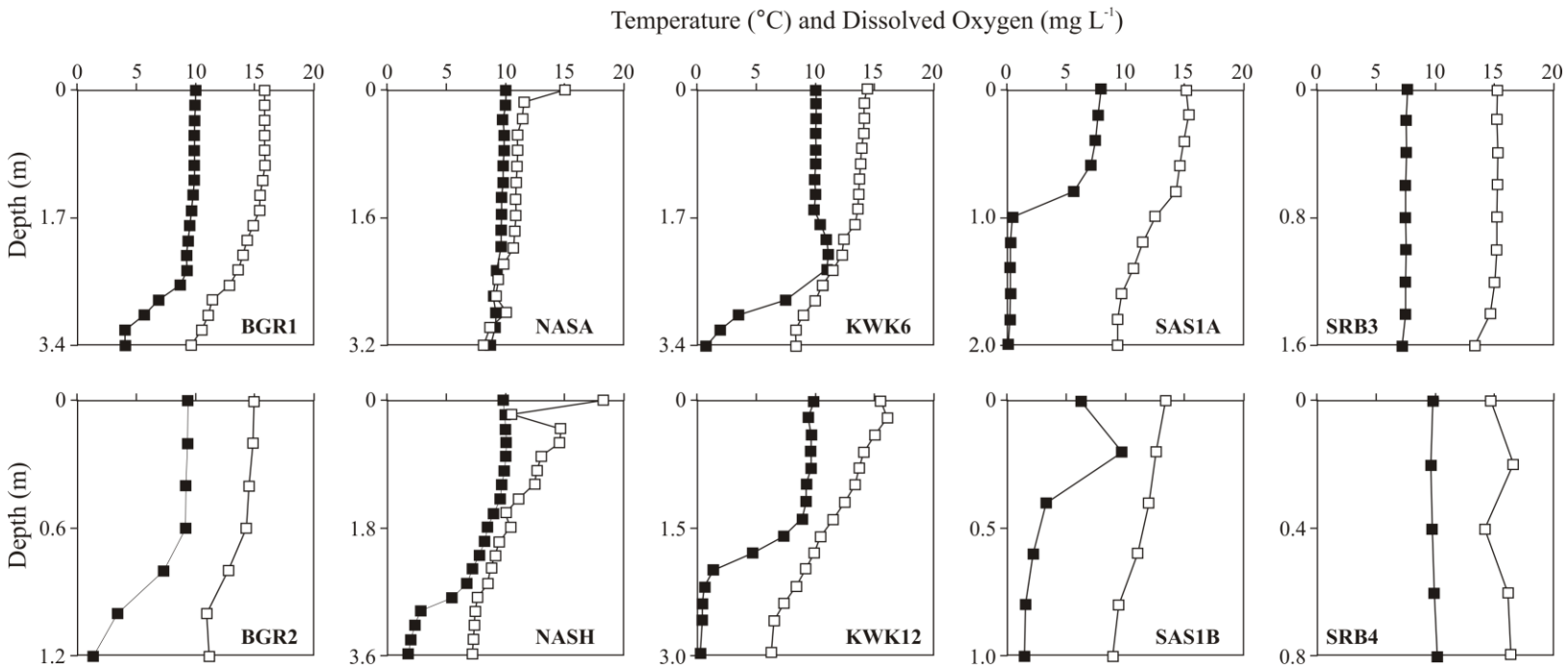

Figure 2. Temperature (white squares) and oxygen (black squares) stratification in the permafrost thaw lakes (BGR, KWK, NAS, SAS) and shallow rock-basin lakes (SRB) in summer 2012.

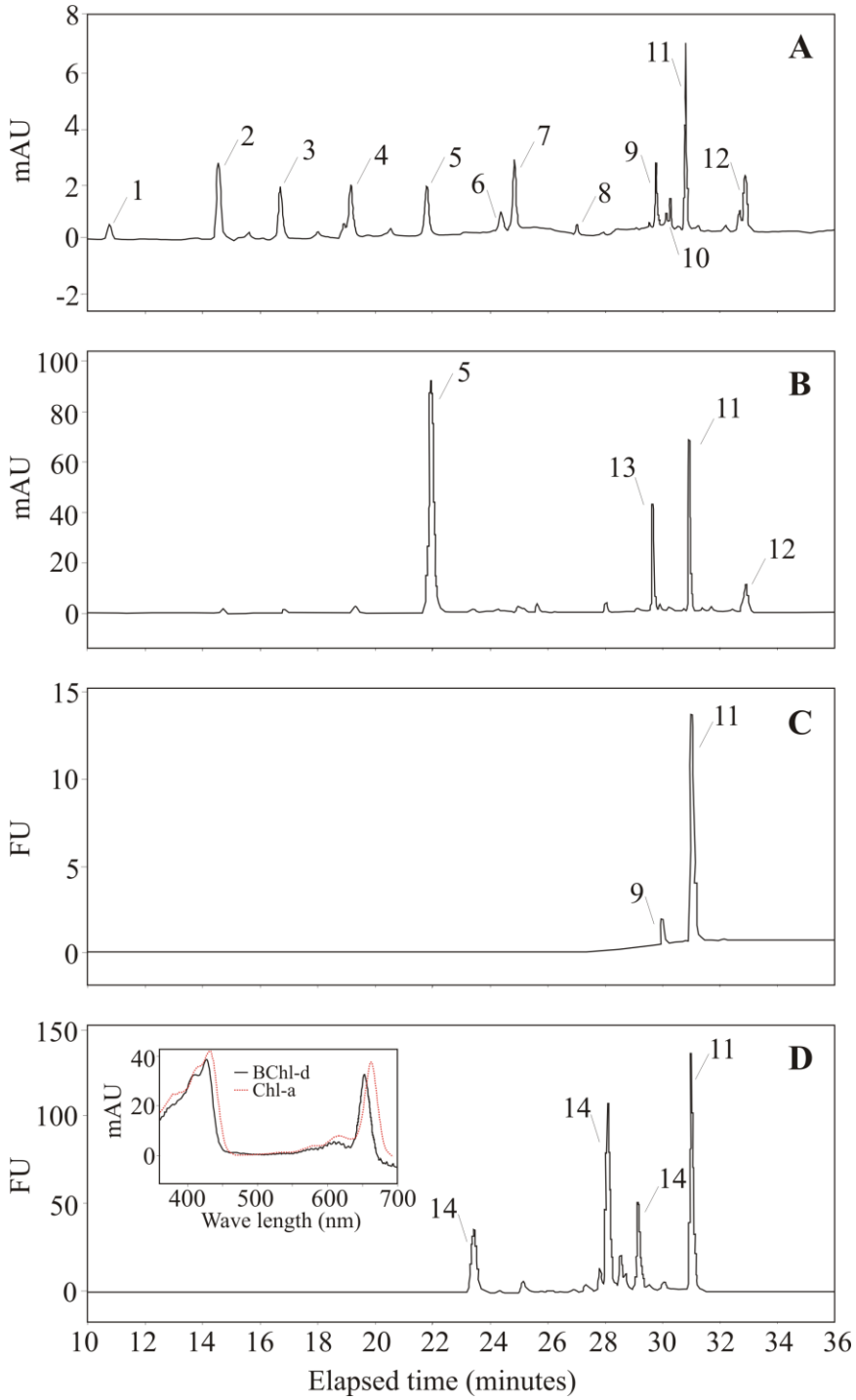

Figure 3. High-performance liquid chromatograms of KWK12 sampled on 3 August 2012: absorbance for the surface (A) or bottom (B) water layers and fluorescence for the surface (C) or bottom (D) water layers (FU = fluorescence units). Pigments from left to right: 1. Perid, 2. Fuco, 3. Viola, 4. Diadino, 5. Allo, 6. Zea, 7. Lut, 8. Cantha, 9. Chl *b*, 10. Echin, 11. Chl *a*, 12. β,β-Carotene, 13. Croco and 14. BChl *d*. Insert in panel D: Bacteriochlorophyll Chl *d* (BCHl *d*, black line) and Chl *a* (red line) absorption spectra (mAU = measured absorption units).

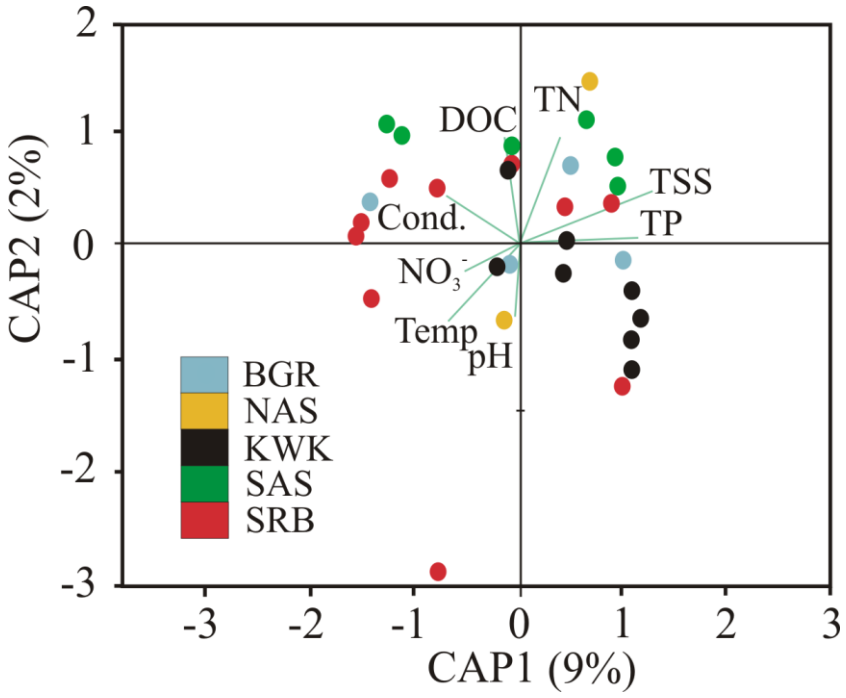

Figure 4. Multivariate analysis by db-RDA of phototrophic pigment composition in the thaw and SRB lakes. Each circle represents individual lakes. The labelled lines represent the significant environmental vectors resulting from correlation analysis.

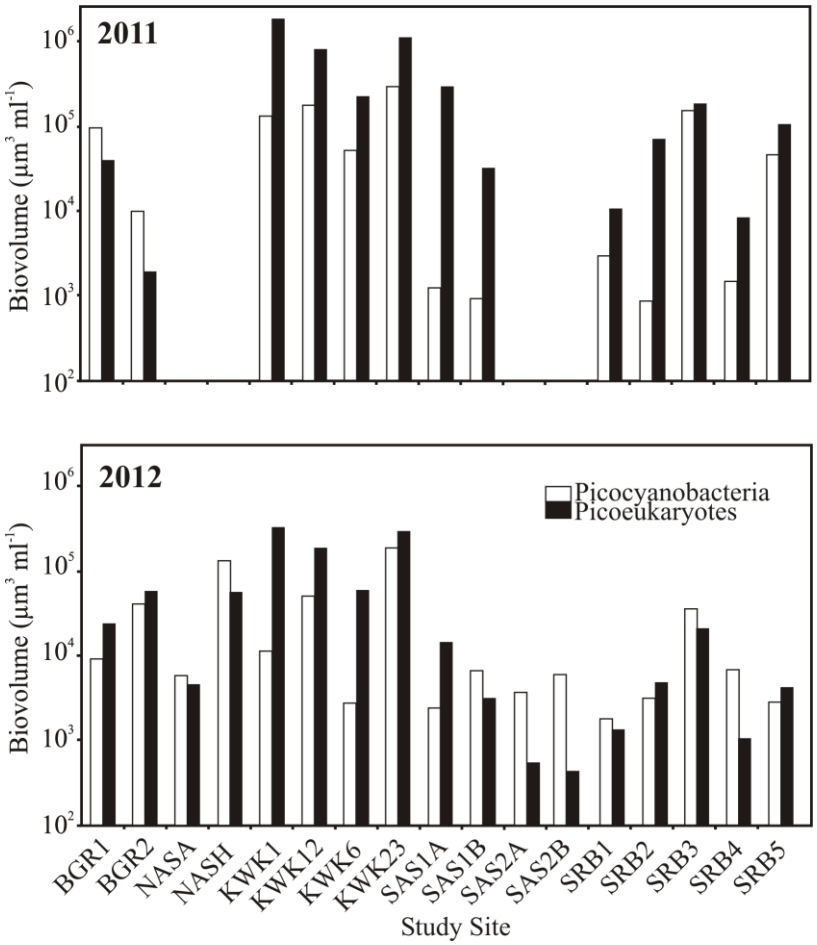

Figure 5. Picophytoplankton biovolume in the surface water of shallow rock-basin (SRB) and permafrost thaw lakes located on clays (KWK, BGR, NAS) and peatlands (SAS).

Supplementary material

Table S1. Location (latitude and longitude), maximum depth (Z) of the subarctic lakes and sampling dates. Water was sampled ca. 20 cm below the surface and ca. 20 cm above the maximum depth. The shallow rock basin lakes have been referred elsewhere as follows: WP1 (SRB1), WP2 (SRB2), Olsha (SRB3), 4 KM (SRB4), Iqalusiuvik (SRB5), – no sampling.

Lakes	Latitude	Longitude	Z	Sampling dates	
			(m)	2011	2012
Thaw lakes on northern clay soils					
BGR1	56°36.650'N	76°12.900'W	3.5	20 Aug	9 Aug
BGR2	56°36.632'N	76°12.937'W	1.0	20 Aug	9 Aug
NASA	56°55.434'N	76°22.708'W	3.2	7 Aug	–
NASH	56°55.452'N	76°22.636'W	3.6	7 Aug	–
Thaw lakes on southern clay soils					
KWK1	55°19.890'N	77°30.241'W	2.1	19 Aug	3 Aug
KWK6	55°19.937'N	77°30.117'W	3.2	21 Aug	4 Aug
KWK12	55°19.808'N	77°30.239'W	2.6	19 Aug	3 Aug
KWK23	55°19.947'N	77°30.131'W	3.4	21 Aug	4 Aug
Thaw lakes on peatlands					
SAS1A	55°13.128'N	77°42.477'W	1.9	23 Aug	5 Aug
SAS1B	55°13.143'N	77°42.475'W	1.7	23 Aug	5 Aug
SAS2A	55°13.591'N	77°41.815'W	2.6	–	13 Aug
SAS2B	55°13.600'N	77°41.806'W	2.0	–	13 Aug
Shallow rock-basin lakes					
SRB1	55°16.982'N	77°44.187'W	0.4	24 Aug	11 Aug
SRB2	55°16.970'N	77°44.122'W	0.8	24 Aug	11 Aug
SRB3	55°16.958'N	77°44.387'W	1.6	24 Aug	14 Aug
SRB4	55°19.907'N	77°41.959'W	0.7	16 Aug	8 Aug
SRB5	55°22.262'N	77°37.072'W	1.8	12 Aug	8 Aug